Supramolecular Chemistry

Multi-functional, Low Symmetry Pd_2L_4 Nanocage Libraries**

James E. M. Lewis*[a]

Abstract: Although many impressive metallo-supramolecular architectures have been reported, they tend towards high symmetry structures and avoid extraneous functionality to ensure high fidelity in the self-assembly process. This minimalist approach, however, limits the range of accessible structures and thus their potential applications. Herein is described the synthesis of a family of ditopic ligands wherein the ligand scaffolds are both low symmetry and incorporate exohedral functional moieties. Key to this design is the use of Cu^I-catalysed azide-alkyne cycloaddition (CuAAC) chemistry, as the triazole is capable of acting as both a coordinating heterocycle and a tether between the ligand framework and functional unit simultaneously. A common precursor was used to generate ligands with various functionalities, allowing control of electronic properties whilst maintaining the core structure of the resultant *cis*-Pd_2L_4 nanocage assemblies. The isostructural nature of the scaffold frameworks enabled formation of combinatorial libraries from the self-assembly of ligand mixtures, generating a statistical mixture of multi-functional, low symmetry architectures.

Introduction

The self-assembly of metal–organic polyhedra (MOPs)[1] remains a popular tool for supramolecular chemists to generate intricate architectures from minimalist building blocks that have demonstrated myriad functionality.[2] Simplicity of components is advantageous: symmetrical structures mitigate the competing processes of narcissistic (self-recognition) and integrative self-sorting (heteromeric-assembly),[3] whilst minimalist ligands inhibit potentially disruptive effects from functional units. Trading fidelity of assembly for high symmetry and spartan scaffolds, however, limits the scope for developing more sophisticated systems.

Pd_2L_4 molecular cages[4] have become a common class of MOP and, despite the potential impediments, strategies for accessing lower symmetry variants have been reported. Use of steric[5] and geometric[6] parameters has enabled the self-assembly of heteroleptic[7] dipalladium nanocages. Exploiting coordination preferences to generate stable metallo-ligands[8] has allowed mixed-metal architectures[9] to be realised. Work in this group,[10] and by others,[11] has focused on an alternative, underexplored option: the use of low symmetry ligands.[12] Designed such that steric or geometric parameters, or a combination of the two, direct the self-assembly process, exclusive formation of specific cage isomers from a potential mixture can be ensured. Although these concepts have been successfully employed in the formation of reduced-symmetry MOPs, they remain devoid of functionality. Indeed, research into exohedral[13] and endohedral[14] functionalisation of ligand scaffolds for MOPs altogether remains relatively scarce.

The 1,2,3-triazole, most commonly synthesised using the Cu^I-catalysed azide-alkyne cycloaddition (CuAAC) reaction,[15] has become a ubiquitous unit in supramolecular chemistry.[16] In addition to being the coordinating unit in readily accessible ligands for MOPs,[17] the specificity of the CuAAC reaction makes the triazole ideal as a benign linker between coordinating and functional moieties.[18] Routinely utilised in either of these roles, the function of the triazole is usually determined at an early stage in the design process. Furthermore, the ability of the triazole to fulfil both of these mandates simultaneously is rarely exploited.

This report details the use of asymmetric, mixed-heterocycle ditopic ligands, with isoquinoline and 1,2,3-triazole coordinating units, for the formation of functionalised *cis*-Pd_2L_4 architectures. Introduction of the triazole unit as the final step in the ligand synthesis enables derivatization of a common precursor, allowing tuning of ligand properties whilst maintaining the structure of the framework core. This structural consistency was able to be exploited in the assembly of mixed-ligand combinatorial cage libraries.

Results and Discussion

Based on principles delineated from earlier work,[10] ligand $\mathbf{L^R}$ (Scheme 1 a), envisaged to be derived from an azide precursor,

[a] *Dr. J. E. M. Lewis*
Department of Chemistry, Imperial College London
Molecular Sciences Research Hub, 82 Wood Lane, London W12 0BZ (UK)
E-mail: james.lewis@imperial.ac.uk

[**] *A previous version of this manuscript has been deposited on a preprint server (https://doi.org/10.26434/chemrxiv.13246715.v1).*

Supporting Information and the ORCID identification number(s) for the author(s) of this article can be found under: https://doi.org/10.1002/chem.202005363.

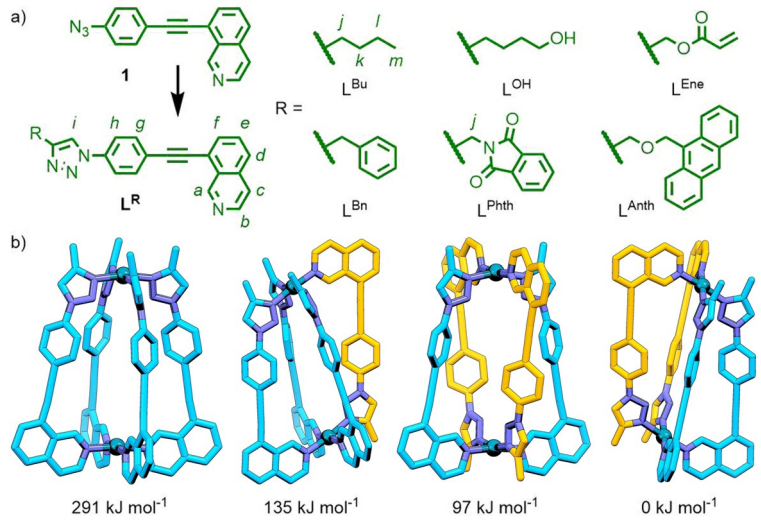

Scheme 1. a) Synthesis of ligands $\mathbf{L^R}$ from azide precursor **1**. b) Geometry optimised structures (PM6) of the four potential $[Pd_2(\mathbf{L^{Me}})_4]^{4+}$ isomers and their relative energies (from left to right: "all-up", "three-up-one-down", *trans* and *cis*). Orange and blue colouring denotes relative ligand orientation.

was designed incorporating both isoquinoline and triazole coordinating units. Optimised models from semi-empirical calculations (PM6) of the four potential $[Pd_2\mathbf{L}_4]^{4+}$ cage isomers assembled from the hypothetical $\mathbf{L^{Me}}$ (where R = CH_3) indicated that the *cis*-Pd_2L_4 isomer would be lowest in energy (Scheme 1 b), consistent with previous computational and experimental work,[11] and from a simple visual analysis appeared to be the most favourable structure. Furthermore, the optimised structure of the *cis* isomer displayed no disquieting distortions of common structural parameters, such as N–Pd–N (≈176°) or alkyne (≈179°) angles, to suggest its formation would be unfavourable.

Buoyed by these rudimentary computational results, the ligand precursor **1** was prepared in 86% overall yield from commercially available reagents (see Supporting Information for details). Submission of **1** to standard CuAAC reaction conditions ($CuSO_4{\cdot}5H_2O$, sodium ascorbate, DMF, RT) with 1-hexyne gave $\mathbf{L^{Bu}}$ in 89% yield.

Pleasingly, a 2:1 combination of $\mathbf{L^{Bu}}$ with $[Pd(CH_3CN)_4](BF_4)_2$ in [D_6]DMSO resulted in a sharp ^{1}H NMR spectrum composed of a single set of signals (Figure 1 a). The combination of downfield shifts of isoquinoline (H_a and H_b; $\Delta\delta = 0.50$ and 1.25 ppm, respectively) and triazole (H_i; $\Delta\delta = 0.37$ ppm) signals in the ^{1}H NMR spectrum (Figure S42), calculated solvodynamic radius (R_S; 9.7 Å) from diffusion-ordered NMR spectroscopy (DOSY; $D = 1.03\times10^{-10}$ m^2s^{-1}), and signals observed by mass spectrometry (MS; Figure 1 b) all indicated formation of a species with formula $[Pd_2(\mathbf{L^{Bu}})_4]^{4+}$. The symmetry of the ^{1}H NMR spectrum and cross-peaks observed by NOESY (H_b···H_j; Figure 1 c) determined that either the *cis* or *trans* isomer had been obtained. Diastereotopic splitting of methylene units of the butyl chain (H_j and H_k) suggested that the *cis* isomer was most likely to have formed. Ultimately, unambiguous confirmation of the *cis*-$[Pd_2(\mathbf{L^{Bu}})_4]^{4+}$ structure came from solid-state single-crystal X-ray diffraction (SCXRD) data (Figure 1 d and e).

Having shown that the ligand framework was indeed suitable for the specific formation of *cis*-Pd_2L_4 structures, a number of ligands derived from the common precursor **1** were prepared (Scheme 1 a). In addition to alkyl substituents, self-assembly of the ligand framework with Pd^{II} was found to be compatible with aryl ($\mathbf{L^{Bn}}$) and bulkier aromatic ($\mathbf{L^{Anth}}$) and heterocyclic ($\mathbf{L^{Phth}}$) moieties, as well as substituents containing heteroatoms ($\mathbf{L^{OH}}$) and unsaturated units ($\mathbf{L^{Ene}}$). Although no SCXRD structures of these cages were obtained, similar MS and NMR spectroscopic details (see Supporting Information) indicated no alteration in the preference for formation of *cis*-Pd_2L_4 cage isomers. With the core *cis*-Pd_2L_4 framework re-

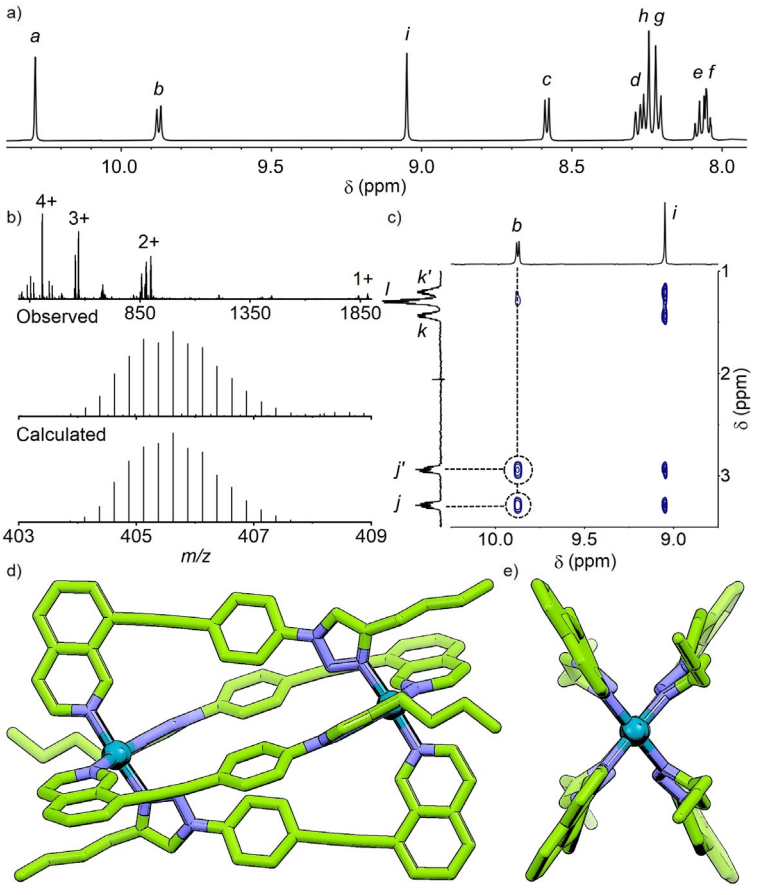

Figure 1. a) Partial ^{1}H NMR spectrum (500 MHz, [D_6]DMSO, 298 K) of $[Pd_2(\mathbf{L^{Bu}})_4](BF_4)_4$; b) MS with observed and calculated peak for $[Pd_2(\mathbf{L^{Bu}})_4]^{4+}$; c) partial NOESY spectrum showing through-space interactions between isoquinoline H_b and butyl chain H_j signals (for signal labelling see Scheme 1); SCXRD structure of $[Pd_2(\mathbf{L^{Bu}})_4](BF_4)_4$ shown d) from the side, and e) down the Pd-Pd axis. N–Pd bond lengths 2.022–2.032 Å; N–Pd–N angles 176.2–176.3°; Pd···Pd distance 11.1 Å. Counterions, solvent molecules and hydrogen atoms omitted for clarity.

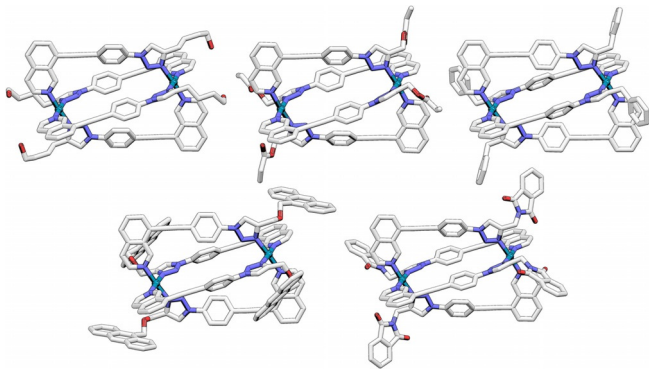

Figure 2. Optimised structures (PM6) of *cis*-$[Pd_2(L^R)_4]^{4+}$ cages assembled from (clockwise from top left) L^{OH}, L^{Ene}, L^{Bn}, L^{Phth} and L^{Anth}. Hydrogen atoms omitted for clarity.

maining isostructural amongst the ligands examined (Figure 2), the ability to use the triazole substituents to modify the properties of the assemblies was investigated.

Although generally considered to be weaker ligands than pyridines, the electronic properties of 1,2,3-triazoles can be tuned with precision through varying the C- and N-substituents.[19] The potential for fine tuning the ligand strength of triazoles in metallo-supramolecular systems, however, is largely overlooked.[20] Within the current system, modulation of donor strength was demonstrated through a comparison of the self-assembly profiles of ligands L^{Bu} and L^{Phth} incorporating electron-donating and -withdrawing groups, respectively.

Titration of Pd^{II} into a [D_6]DMSO solution of L^{Phth} (Figure 3a) resulted in formation of the expected $[Pd_2(L^{Phth})_4]^{4+}$ cage when a 1:2 metal/ligand ratio was reached (Figure 3c). At a 1:4 ratio, however, a single species was observed (Figure 3b) that was spectroscopically distinct from both the free ligand and Pd_2L_4

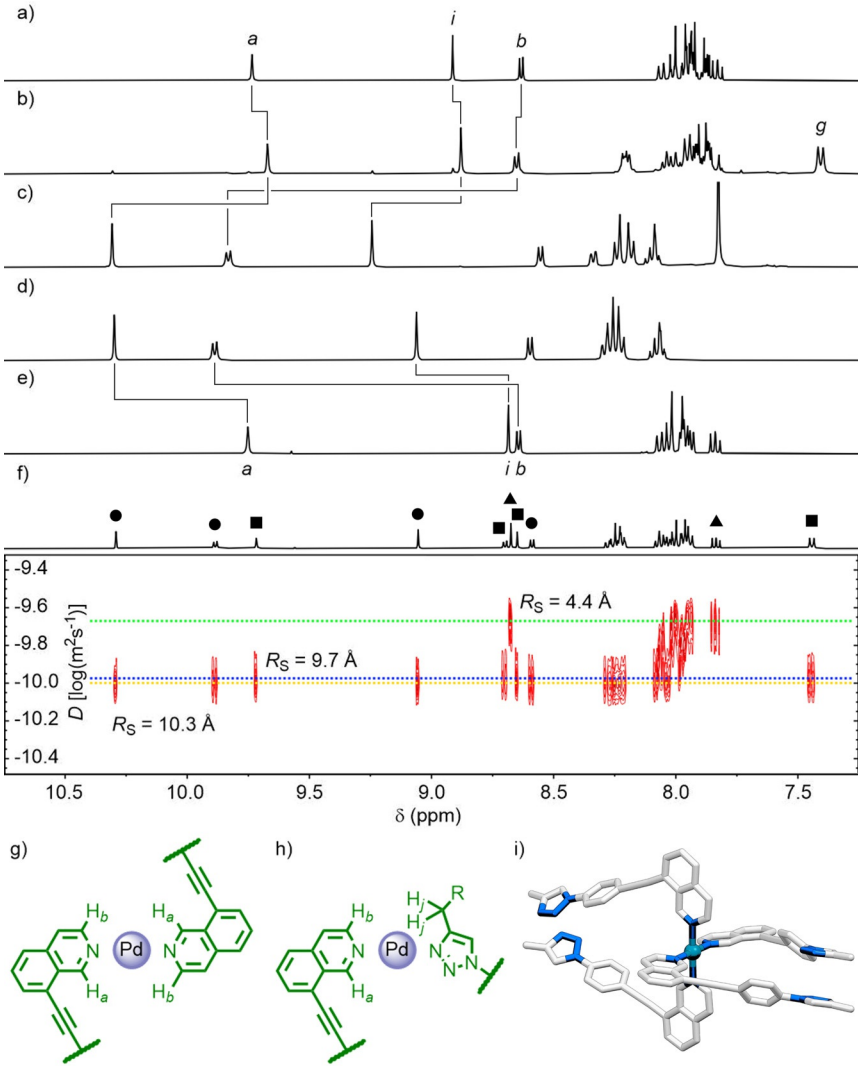

Figure 3. Controlling the self-assembly profile of L^R through tuning the electronic properties of the triazole. Partial ^{1}H NMR spectra (400 MHz, [D_6]DMSO, 298 K) of a) L^{Phth}, b) L^{Phth} + 0.25 equiv. Pd^{II}, c) L^{Phth} + 0.50 equiv. Pd^{II}, d) L^{Bu} + 0.50 equiv. Pd^{II}, and e) L^{Bu}. For signal labelling see Scheme 1. f) Partial DOSY spectrum (500 MHz, [D_6]DMSO, 298 K) of L^{Bu} + 0.25 equiv. Pd^{II}. Non-overlapping peaks have been assigned where possible as $[Pd_2(L^{Bu})_4]^{4+}$ (●), $[Pd(L^{Bu})_4]^{2+}$ (■), and L^{Bu} (▲). Chemical structures showing indicative through-space interactions between protons for g) mononuclear $[Pd(L^R)_4]^{2+}$ species and h) $[Pd_2(L^R)_4]^{4+}$ cage assemblies. i) Molecular model of one possible conformation of a mononuclear $[Pd(L^{Me})_4]^{2+}$ structure with coordination exclusively through the isoquinoline units.

cage, although DOSY suggested that it was of a similar size to the latter ($R_S \approx 11$ Å, compared to 11.3 Å for the cage). The NOESY spectrum (Figure S109) revealed cross-peaks between H_a and H_b of the isoquinoline, which would only be expected were at least two of these heterocycles to be brought into close proximity through coordination in an anti-parallel fashion (Figure 3g); in contrast to the cage, *cis*-$[Pd_2(\mathbf{L}^{\mathbf{Phth}})_4]^{4+}$, no interactions between H_b of the isoquinoline and H_j of the triazole substituent were observed (Figure 3h). These data are consistent with the formation of a mononuclear complex, $[Pd(\mathbf{L}^{\mathbf{Phth}})_4]^{2+}$, with coordination to the Pd^{II} ions occurring through the isoquinoline units (a molecular model of one possible conformer of a hypothetical model complex, $[Pd(\mathbf{L}^{\mathbf{Me}})_4]^{2+}$, is shown in Figure 3i).

Additional support for the identity of the mononuclear species came from a model compound, namely the complex formed from the self-assembly of monodentate ligand precursor **1**. A 4:1 mixture of **1** with Pd^{II} yielded a sharp set of signals (Figure S113) wherein characteristic peaks—H_a, H_b and H_g—resonated at similar chemical shifts to those observed for the purported $[Pd(\mathbf{L}^{\mathbf{Phth}})_4]^{2+}$ complex. Unfortunately, no signals for this latter species were observed by MS (although an isotopic pattern consistent with the formula $\{[Pd(\mathbf{L}^{\mathbf{Phth}})_3](X^-)\}^+$ (Figure S111) could be seen), presumably due to the instability of the mononuclear complex under the ESI-MS conditions. SCXRD data was obtained, however, that confirmed the anticipated structure of the model complex, $[Pd(\mathbf{1})_4]^{2+}$ (Figure S130).[21]

The situation with $\mathbf{L}^{\mathbf{Bu}}$ was slightly more complex. The ^{1}H NMR spectrum obtained from a 1:4 mixture of Pd^{II} and $\mathbf{L}^{\mathbf{Bu}}$ (Figure 3f) at first glance appeared to indicate a stoichiometric mixture of $[Pd_2(\mathbf{L}^{\mathbf{Bu}})_4]^{4+}$ (Figure 3d) and free $\mathbf{L}^{\mathbf{Bu}}$ (Figure 3e). Closer inspection revealed additional peaks, belonging to neither of these species, that resembled the mononuclear complex seen with $\mathbf{L}^{\mathbf{Phth}}$. This suggested that these three species ($\mathbf{L}^{\mathbf{Bu}}$, $[Pd(\mathbf{L}^{\mathbf{Bu}})_4]^{2+}$ and $[Pd_2(\mathbf{L}^{\mathbf{Bu}})_4]^{4+}$) might all be present in solution.

2D NMR—in particular NOESY and DOSY—was used to assign non-overlapping signals to individual components of this mixture. In the NOESY spectrum (Figure S106) cross-peaks indicative of $H_b \cdots H_j$ interactions between the isoquinoline and butyl chain (Figure 3h) could be seen for the cage assembly but were absent for those signals assigned to the mononuclear complex; additionally, $H_a \cdots H_b$ interactions could be seen for the latter (Figure 3g). DOSY (Figure 3f) showed peaks assigned to the cage and mononuclear complexes to be diffusing at similar rates ($D = 10.0$ and 9.8×10^{-11} $m^2 s^{-1}$, respectively) whilst those assumed to be from the free ligand diffused much quicker ($D = 4.4 \times 10^{-11}$ $m^2 s^{-1}$), indicative of two similarly sized species and one much smaller ($R_S = 10.3$, 9.7 and 4.4 Å, respectively) being present in solution.

Thus, based on the spectral data, it was concluded that a 1:4 mixture of Pd^{II} and $\mathbf{L}^{\mathbf{Bu}}$ generated a combination of the dinuclear cage, mononuclear complex (with coordination again presumed to be through the isoquinoline units) and free ligand. It is noted that for free $\mathbf{L}^{\mathbf{Bu}}$, downfield signals associated with protons H_a and H_b adjacent to the nitrogen atom of the isoquinoline could not be identified. It is assumed that these peaks had broadened significantly, possibly due to transient non-covalent interactions with the $[Pd_2(\mathbf{L}^{\mathbf{Bu}})_4]^{4+}$ and/or $[Pd(\mathbf{L}^{\mathbf{Bu}})_4]^{2+}$ complexes.

The proton affinity (PA) of N3 of the triazole, as determined by DFT calculations (B3LYP-6-31G(d)), was increased by 16 kJ mol^{-1} going from the electron-withdrawing *N*-methylenephthalimide substituent in $\mathbf{L}^{\mathbf{Phth}}$ to the electron-donating butyl group of $\mathbf{L}^{\mathbf{Bu}}$ (see Supporting Information for details). Using PA as a proxy for ligand strength, these results support the rationalisation of the observed differences in self-assembly as arising from differences in the σ-donor ability of the triazoles between the two ligands. The combined experimental and computational results demonstrate effective control of the ligand framework's electronic properties, through tailoring of the triazole substituent, without ultimately affecting the core structure of the *cis*-Pd_2L_4 assembly.

Since the core framework remained constant between the different functionalised ligands, it seemed that it would be possible to generate a statistical combinatorial library of homoleptic and mixed-ligand cages through self-assembly of a mixture of more than one ligand.[22] To examine this, Pd^{II} and a binary mixture of $\mathbf{L}^{\mathbf{Bu}}$ and either $\mathbf{L}^{\mathbf{Bn}}$ or $\mathbf{L}^{\mathbf{Phth}}$ were combined in a 1:1:1 ratio in [D_6]DMSO. The resultant self-assembled libraries gave well-defined ^{1}H NMR spectra (Figures 4b and S115) that appeared to contain multiple overlapping signals from species of a similar size to the homoleptic assemblies ($R_S \approx 10$–11 Å). These mixtures were found to be composed of the five possible homoleptic and heteroleptic constitutional assemblies with the formula $[Pd_2(\mathbf{L}^{\mathbf{Bu}})_x(\mathbf{L}^{\mathbf{Bn}}/\mathbf{L}^{\mathbf{Phth}})_{(4-x)}]^{4+}$ (Figure 4d) by MS (Figure 4e).

It is noted that whilst the homoleptic and *cis*-$Pd_2\mathbf{L}^{\mathbf{1}}{}_3\mathbf{L}^{\mathbf{2}}$-type architectures should be present as single diastereomers, *cis*-$Pd_2\mathbf{L}^{\mathbf{1}}{}_2\mathbf{L}^{\mathbf{2}}{}_2$ assemblies with asymmetric ligands have the potential to exist as three different diastereomeric forms depending on the relative arrangements and orientations of the ligands (Figure 4d), although these isomers cannot be distinguished by MS. Additionally, the two $Pd_2\mathbf{L}^{\mathbf{1}}{}_3\mathbf{L}^{\mathbf{2}}$ and one of the $Pd_2\mathbf{L}^{\mathbf{1}}{}_2\mathbf{L}^{\mathbf{2}}{}_2$ cages are chiral, resulting in a library of ten cages in total. Herein the three $Pd_2\mathbf{L}^{\mathbf{1}}{}_2\mathbf{L}^{\mathbf{2}}{}_2$ cage isomers have been termed *syn*, *cis-anti* and *trans-anti*, where for pairs of the same ligand (in this instance for example, the pair of $\mathbf{L}^{\mathbf{Bu}}$ ligands) *syn*/*anti* denotes parallel/antiparallel relative orientations, and *cis*/*trans* indicates their relative positions within the *cis*-Pd_2L_4 structure (i.e. adjacent or opposite from each other, respectively).

Having successfully demonstrated statistical mixing of a binary combination of ligands, a ternary system was subsequently examined. $\mathbf{L}^{\mathbf{OH}}$, $\mathbf{L}^{\mathbf{Phth}}$ and $\mathbf{L}^{\mathbf{Anth}}$ were combined with Pd^{II} in a 2:2:2:3 ratio in [D_6]DMSO. Unsurprisingly, the resultant ^{1}H NMR spectrum was somewhat complex (Figure S123). The DOSY data, however, were consistent with the formation of appropriately sized assemblies ($R_S = 11.0$ Å). The MS data was more complex than for previous systems, likely due to overlapping signals from the multitude of species present in solution, and anion exchange under the MS conditions. However, signals congruent with the three possible tris-heteroleptic assemblies (i.e., those incorporating at least one of each ligand) were observed (Figure S125). Signals consistent with most of the 15 ex-

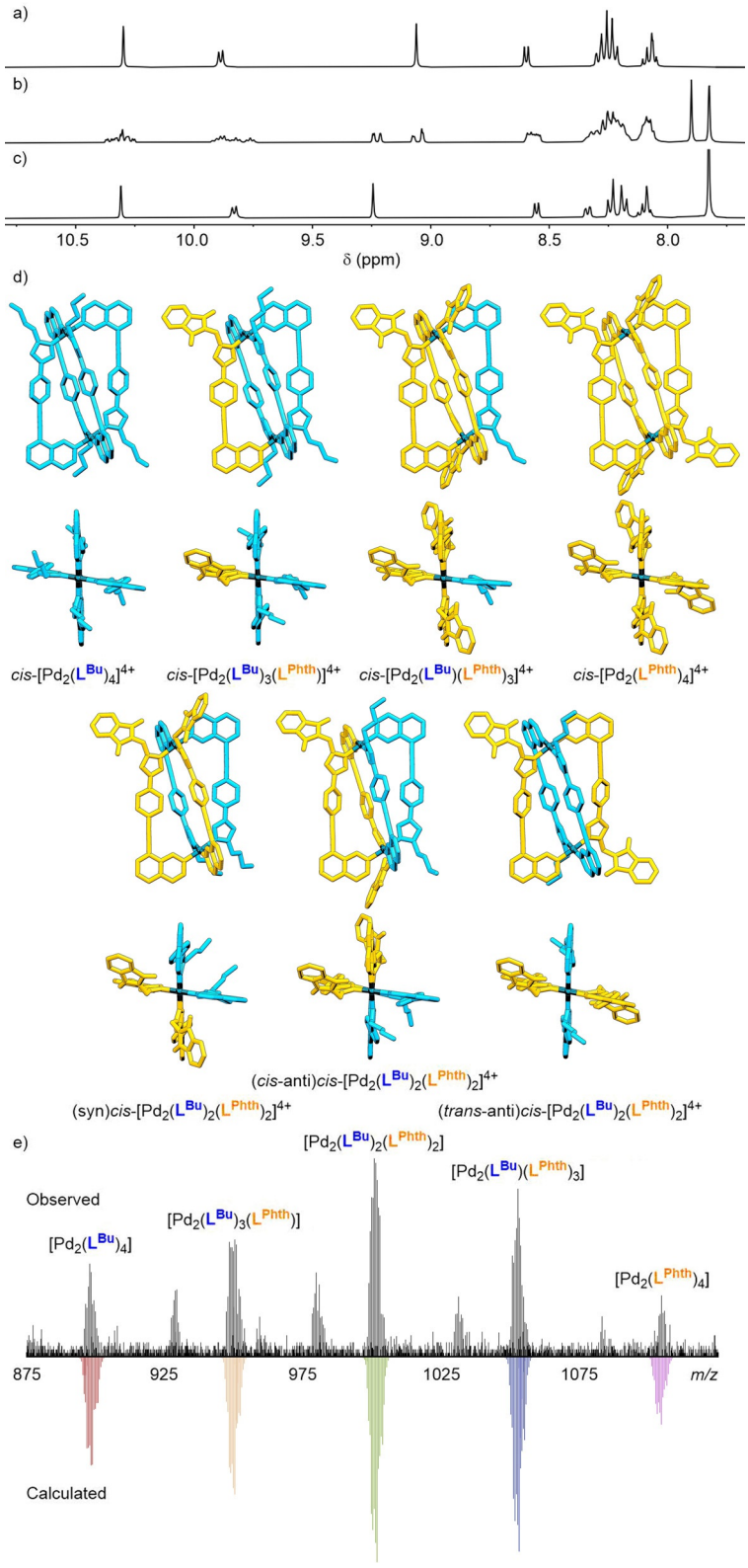

Figure 4. Partial ^{1}H NMR spectra (400 MHz, [D_6]DMSO, 298 K) of a) $[Pd_2(\mathbf{L}^{Bu})_4](BF_4)_4$, b) combinatorial library $[Pd_2(\mathbf{L}^{Bu})_x(\mathbf{L}^{Phth})_{(4-x)}](BF_4)_4$, and c) $[Pd_2(\mathbf{L}^{Phth})_4](BF_4)_4$. d) Optimised structures (PM6) of the members of the combinatorial library $[Pd_2(\mathbf{L}^{Bu})_x(\mathbf{L}^{Phth})_{(4-x)}]^{4+}$ including the three diastereomeric forms of $[Pd_2(\mathbf{L}^{Bu})_2(\mathbf{L}^{Phth})_2]^{4+}$ (single enantiomers of chiral cages shown). $\mathbf{L}^{Bu}$ and $\mathbf{L}^{Phth}$ ligands have been coloured blue and orange, respectively. e) Observed MS and calculated signals for $\{[Pd_2(\mathbf{L}^{Bu})_x(\mathbf{L}^{Phth})_{(4-x)}](BF_4)_2\}^{2+}$ ions (x = 0–4).

pected constitutional assemblies of the library could also be seen (Figure 5). As several of the bis-heteroleptic and all of the tris-heteroleptic assemblies are expected to exist as a mixture of diastereomers, and a number of these are chiral, the combinatorial library is considered to consist of a total of 45 *cis*-Pd_2L_4 cages (Figure S128).

Conclusions

A family of asymmetric, ditopic ligands that self-assemble into exohedrally functionalised, low symmetry *cis*-Pd_2L_4 architectures was realised. CuAAC chemistry was employed to yield these mixed-heterocycle ligands in which a 1,2,3-triazole unit served as both a coordinating unit and linker to append functional groups to the assembly scaffold. A variety of functional groups were shown to be tolerated without impacting the core structure of the cage. Furthermore, facile tuning of electronic properties was demonstrated, allowing modification of the ligand self-assembly profile. Due to the isostructural nature of the core framework of the ligands, and their resultant Pd_2L_4 assemblies, it was shown possible to generate combinatorial libraries that included mixed-ligand architectures with multiple functional moieties. With the need to move towards more complex MOPs to advance their utility in various applications, this study has demonstrated an underexplored approach to readily access functional, low symmetry metal–organic assemblies.

Experimental Section

Crystal data for $[Pd_2(\mathbf{L}^{Bu})_4](BF_4)_4$: $Pd_2(C_{23}H_{20}N_4)_4(BF_4)_4{\cdot}2(C_6H_{14}O){\cdot}4(C_3H_7NO)$, M = 2466.48, monoclinic, $P2_1/n$, a = 13.4683(3), b = 18.1293(4), c = 24.7113(5) Å, α = 90, β = 99.400(2), γ = 90°, V = 5952.8(2) Å^3, Z = 2, ρ_{cald} = 1.376 mg m^{-3}, $\mu(Mo_{K\alpha})$ = 0.389 mm^{-1}, T = 173 K, 12454 independent measured reflections (R_{int} = 0.0322), R_1 = 0.0752, $wR2$ = 0.2057 [$I > 2\sigma(I)$], completeness = 99.7, 689 parameters, GOF on F^2 = 1.032, max/min residual density 1.859/−0.998 e Å^{-3}. Deposition Number 2043240 contains the supplementary crystallographic data for this paper. These data are provided free of charge by the joint Cambridge Crystallographic Data Centre and Fachinformationszentrum Karlsruhe Access Structures service www.ccdc.cam.ac.uk/structures.

$\mathbf{L}^{R}$ were prepared according to the following general procedure: **1** (67.6 mg, 0.25 mmol), $CuSO_4{\cdot}5H_2O$ (31.2 mg, 0.125 mmol), sodium ascorbate (49.5 mg, 0.25 mmol) and appropriate alkyne were stirred at RT in DMF (5 mL) for 16 h. The reaction mixture was diluted with EtOAc (40 mL) and washed with 0.1 M EDTA-Na_2 in 1:9 $NH_4OH_{(aq)}/H_2O$ (10 mL), brine (4×10 mL), dried ($MgSO_4$) and the solvent removed *in vacuo*, with subsequent purification by column chromatography on silica gel.

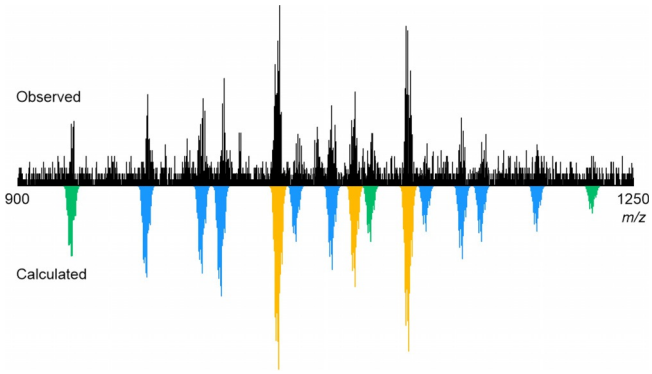

Figure 5. Partial MS of the ternary combinatorial library with calculated signals for $\{[Pd_2L_4](BF_4)_2\}^{2+}$ ions with one (green), two (blue), and three (orange) different ligands.

$[Pd_2(\mathbf{L^R})_4](BF_4)_4$ were prepared by sonicating $\mathbf{L^R}$ (0.030 mmol) and $[Pd(CH_3CN)_4](BF_4)_2$ (6.7 mg, 0.015 mmol) in [D$_6$]DMSO (0.75 mL) until a homogenous solution was obtained.

For calculated structures in *xyz* format see DOI: https://doi.org/10.14469/hpc/7366.

Acknowledgements

This work was supported by an Imperial College Research Fellowship. Thanks to Peter Haycock and Corey Fulop for assistance with the collection of NMR data, Dr. Lisa Haigh for MS data, Dr. Andrew White for collection of SCXRD data, Dr. Dan Preston for useful discussions, and Prof. Matthew Fuchter for useful discussions and access to equipment and resources.

Conflict of interest

The author declares no conflict of interest.

Keywords: cages · combinatorial library · metallosupramolecular · self-assembly · asymmetrical

[1] a) M. Fujita, *Chem. Soc. Rev.* **1998**, *27*, 417–425; b) S. Leininger, B. Olenyuk, P. J. Stang, *Chem. Rev.* **2000**, *100*, 853–908; c) B. J. Holliday, C. A. Mirkin, *Angew. Chem. Int. Ed.* **2001**, *40*, 2022–2043; *Angew. Chem.* **2001**, *113*, 2076–2097; d) M. D. Ward, *Chem. Commun.* **2009**, 4487–4499; e) R. Chakrabarty, P. S. Mukherjee, P. J. Stang, *Chem. Rev.* **2011**, *111*, 6810–6918; f) M. M. J. Smulders, I. A. Riddell, C. Browne, J. R. Nitschke, *Chem. Soc. Rev.* **2013**, *42*, 1728–1754; g) T. K. Ronson, S. Zarra, S. P. Black, J. R. Nitschke, *Chem. Commun.* **2013**, *49*, 2476–2490; h) T. R. Cook, P. J. Stang, *Chem. Rev.* **2015**, *115*, 7001–7045; i) N. B. Debata, D. Tripathy, H. S. Sahoo, *Coord. Chem. Rev.* **2019**, *387*, 273–298.

[2] a) M. Yoshizawa, J. K. Klosterman, M. Fujita, *Angew. Chem. Int. Ed.* **2009**, *48*, 3418–3438; *Angew. Chem.* **2009**, *121*, 3470–3490; b) T. R. Cook, V. Vajpayee, M. H. Lee, P. J. Stang, K. W. Chi, *Acc. Chem. Res.* **2013**, *46*, 2464–2474; c) B. Therrien, *Chem. Eur. J.* **2013**, *19*, 8378–8386; d) C. J. Brown, F. D. Toste, R. G. Bergman, K. N. Raymond, *Chem. Rev.* **2015**, *115*, 3012–3035; e) A. Casini, B. Woods, M. Wenzel, *Inorg. Chem.* **2017**, *56*, 14715–14729; f) T. Y. Kim, R. A. S. Vasdev, D. Preston, J. D. Crowley, *Chem. Eur. J.* **2018**, *24*, 14878–14890; g) I. Sinha, P. S. Mukherjee, *Inorg. Chem.* **2018**, *57*, 4205–4221; h) Y. Fang, J. A. Powell, E. Li, Q. Wang, Z. Perry, A. Kirchon, X. Yang, Z. Xiao, C. Zhu, L. Zhang, F. Huang, H.-C. Zhou, *Chem. Soc. Rev.* **2019**, *48*, 4707–4730; i) H. Sepehrpour, W. Fu, Y. Sun, P. J. Stang, *J. Am. Chem. Soc.* **2019**, *141*, 14005–14020; j) F. J. Rizzuto, L. K. S. von Krbek, J. R. Nitschke, *Nat. Rev. Chem.* **2019**, *3*, 204–222; k) E. J. Gosselin, C. A. Rowland, E. D. Bloch, *Chem. Rev.* **2020**, *120*, 8987–9014; l) Y. Xue, X. Hang, J. Ding, B. Li, R. Zhu, H. Pang, Q. Xu, *Coord. Chem. Rev.* **2020**, 213656.

[3] a) Z. He, W. Jiang, C. A. Schalley, *Chem. Soc. Rev.* **2015**, *44*, 779–789; b) L. R. Holloway, P. M. Bogie, R. J. Hooley, *Dalton Trans.* **2017**, *46*, 14719–14723; c) W. M. Bloch, G. H. Clever, *Chem. Commun.* **2017**, *53*, 8506–8516.

[4] For selected examples see: a) D. A. McMorran, P. J. Steel, *Angew. Chem. Int. Ed.* **1998**, *37*, 3295–3297; *Angew. Chem.* **1998**, *110*, 3495–3497; b) D. K. Chand, K. Biradha, M. Fujita, *Chem. Commun.* **2001**, 1652–1653; c) G. H. Clever, S. Tashiro, M. Shionoya, *Angew. Chem. Int. Ed.* **2009**, *48*, 7010–7012; *Angew. Chem.* **2009**, *121*, 7144–7146; d) J. D. Crowley, E. L. Gavey, *Dalton Trans.* **2010**, *39*, 4035–4037; e) P. Liao, B. W. Langloss, A. M. Johnson, E. R. Knudsen, F. S. Tham, R. R. Julian, R. J. Hooley, *Chem. Commun.* **2010**, *46*, 4932–4934; f) N. Kishi, Z. Li, K. Yoza, M. Akita, M. Yoshizawa, *J. Am. Chem. Soc.* **2011**, *133*, 11438–11441; g) J. E. M. Lewis, E. L. Gavey, S. A. Cameron, J. D. Crowley, *Chem. Sci.* **2012**, *3*, 778–784; h) S. M. Jansze, M. D. Wise, A. V. Vologzhanina, R. Scopelliti, K. Severin, *Chem. Sci.* **2017**, *8*, 1901–1908; i) D. Preston, K. M. Patil, A. T. O'Neil, R. A. S. Vasdev, J. A. Kitchen, P. E. Kruger, *Inorg. Chem. Front.* **2020**, *7*, 2990–3001.

[5] a) D. Preston, J. E. Barnsley, K. C. Gordon, J. D. Crowley, *J. Am. Chem. Soc.* **2016**, *138*, 10578–10585; b) R. Zhu, W. M. Bloch, J. J. Holstein, S. Mandal, L. V. Schäfer, G. H. Clever, *Chem. Eur. J.* **2018**, *24*, 12976–12982.

[6] a) W. M. Bloch, Y. Abe, J. J. Holstein, C. M. Wandtke, B. Dittrich, G. H. Clever, *J. Am. Chem. Soc.* **2016**, *138*, 13750–13755; b) W. M. Bloch, J. J. Holstein, W. Hiller, G. H. Clever, *Angew. Chem. Int. Ed.* **2017**, *56*, 8285–8289; *Angew. Chem.* **2017**, *129*, 8399–8404; c) K. Wu, B. Zhang, C. Drechsler, J. J. Holstein, G. H. Clever, *Angew. Chem. Int. Ed.* **2020**, https://doi.org/10.1002/anie.202012425; *Angew. Chem.* **2020**, https://doi.org/10.1002/ange.202012425.

[7] a) S. Pullen, G. H. Clever, *Acc. Chem. Res.* **2018**, *51*, 3052–3064; b) D. Bardhan, D. K. Chand, *Chem. Eur. J.* **2019**, *25*, 12241–12269.

[8] a) S. Hiraoka, Y. Sakata, M. Shionoya, *J. Am. Chem. Soc.* **2008**, *130*, 10058–10059; b) H. B. Wu, Q. M. Wang, *Angew. Chem. Int. Ed.* **2009**, *48*, 7343–7345; *Angew. Chem.* **2009**, *121*, 7479–7481; c) M. M. J. Smulders, A. Jiménez, J. R. Nitschke, *Angew. Chem. Int. Ed.* **2012**, *51*, 6681–6685; *Angew. Chem.* **2012**, *124*, 6785–6789; d) W. J. Ramsay, T. K. Ronson, J. K. Clegg, J. R. Nitschke, *Angew. Chem. Int. Ed.* **2013**, *52*, 13439–13443; *Angew. Chem.* **2013**, *125*, 13681–13685; e) K. Li, L. Y. Zhang, C. Yan, S. C. Wei, M. Pan, L. Zhang, C. Y. Su, *J. Am. Chem. Soc.* **2014**, *136*, 4456–4459; f) M. D. Wise, J. J. Holstein, P. Pattison, C. Besnard, E. Solari, R. Scopelliti, G. Bricogne, K. Severin, *Chem. Sci.* **2015**, *6*, 1004–1010; g) W. J. Ramsay, F. T. Szczypiński, H. Weissman, T. K. Ronson, M. M. J. Smulders, B. Rybtchinski, J. R. Nitschke, *Angew. Chem. Int. Ed.* **2015**, *54*, 5636–5640; *Angew. Chem.* **2015**, *127*, 5728–5732; h) S. Sanz, H. M. O'Connor, E. M. Pineda, K. S. Pedersen, G. S. Nichol, O. Mønsted, H. Weihe, S. Piligkos, E. J. L. McInnes, P. J. Lusby, E. K. Brechin, *Angew. Chem. Int. Ed.* **2015**, *54*, 6761–6764; *Angew. Chem.* **2015**, *127*, 6865–6868; i) A. J. Metherell, M. D. Ward, *Chem. Sci.* **2016**, *7*, 910–915; j) Y. J. Hou, K. Wu, Z. W. Wei, K. Li, Y. L. Lu, C. Y. Zhu, J. S. Wang, M. Pan, J. J. Jiang, G. Q. Li, C. Y. Su, *J. Am. Chem. Soc.* **2018**, *140*, 18183–18191; k) D. Preston, J. J. Sutton, K. C. Gordon, J. D. Crowley, *Angew. Chem. Int. Ed.* **2018**, *57*, 8659–8663; *Angew. Chem.* **2018**, *130*, 8795–8799; l) M. Hardy, N. Struch, J. J. Holstein, G. Schnakenburg, N. Wagner, M. Engeser, J. Beck, G. H. Clever, A. Lützen, *Angew. Chem. Int. Ed.* **2020**, *59*, 3195–3200; *Angew. Chem.* **2020**, *132*, 3221–3226; m) L. S. Lisboa, J. A. Findlay, L. J. Wright, C. G. Hartinger, J. D. Crowley, *Angew. Chem. Int. Ed.* **2020**, *59*, 11101–11107; *Angew. Chem.* **2020**, *132*, 11194–11200; n) D. Yang, J. L. Greenfield, T. K. Ronson, L. K. S. von Krbek, L. Yu, J. R. Nitschke, *J. Am. Chem. Soc.* **2020**, *142*, 19856–19861.

[9] a) Y. Y. Zhang, W. X. Gao, L. Lin, G. X. Jin, *Coord. Chem. Rev.* **2017**, *344*, 323–344; b) M. Hardy, A. Lützen, *Chem. Eur. J.* **2020**, *26*, 13332–13346.

[10] J. E. M. Lewis, A. Tarzia, A. J. P. White, K. E. Jelfs, *Chem. Sci.* **2020**, *11*, 677–683.

[11] a) S. Hiraoka, M. Fujita, *J. Am. Chem. Soc.* **1999**, *121*, 10239–10240; b) D. Ogata, J. Yuasa, *Angew. Chem. Int. Ed.* **2019**, *58*, 18424–18428; *Angew. Chem.* **2019**, *131*, 18595–18599; c) S. S. Mishra, S. V. K. Kompella, S. Krishnaswamy, S. Balasubramanian, D. K. Chand, *Inorg. Chem.* **2020**, *59*, 12884–12894.

[12] J. E. M. Lewis, J. D. Crowley, *ChemPlusChem* **2020**, *85*, 815 – 827.
[13] For selected examples see: a) N. Kamiya, M. Tominaga, S. Sato, M. Fujita, *J. Am. Chem. Soc.* **2007**, *129*, 3816 – 3817; b) T. Kikuchi, S. Sato, M. Fujita, *J. Am. Chem. Soc.* **2010**, *132*, 15930 – 15932; c) M. Ikemi, T. Kikuchi, S. Matsumura, K. Shiba, S. Sato, M. Fujita, *Chem. Sci.* **2010**, *1*, 68 – 71; d) J. Park, L. B. Sun, Y. P. Chen, Z. Perry, H. C. Zhou, *Angew. Chem. Int. Ed.* **2014**, *53*, 5842 – 5846; *Angew. Chem.* **2014**, *126*, 5952 – 5956; e) J. E. M. Lewis, A. B. S. Elliott, C. J. McAdam, K. C. Gordon, J. D. Crowley, *Chem. Sci.* **2014**, *5*, 1833 – 1843; f) K. K. G. Wong, N. Hoyas Pérez, A. J. P. White, J. E. M. Lewis, *Chem. Commun.* **2020**, *56*, 10453 – 10456.
[14] For selected examples see: a) M. Tominaga, K. Suzuki, T. Murase, M. Fujita, *J. Am. Chem. Soc.* **2005**, *127*, 11950 – 11951; b) S. Sato, J. Iida, K. Suzuki, M. Kawano, T. Ozeki, M. Fujita, *Science* **2006**, *313*, 1273 – 1276; c) K. Suzuki, M. Kawano, S. Sato, M. Fujita, *J. Am. Chem. Soc.* **2007**, *129*, 10652 – 10653; d) K. Suzuki, K. Takao, S. Sato, M. Fujita, *J. Am. Chem. Soc.* **2010**, *132*, 2544 – 2545; e) K. Suzuki, S. Sato, M. Fujita, *Nat. Chem.* **2010**, *2*, 25 – 29; f) D. Fujita, K. Suzuki, S. Sato, M. Yagi-Utsumi, Y. Yamaguchi, N. Mizuno, T. Kumasaka, M. Takata, M. Noda, S. Uchiyama, K. Kato, M. Fujita, *Nat. Commun.* **2012**, *3*, 1093; g) C. J. Bruns, D. Fujita, M. Hoshino, S. Sato, J. F. Stoddart, M. Fujita, *J. Am. Chem. Soc.* **2014**, *136*, 12027 – 12034; h) Y. Ueda, H. Ito, D. Fujita, M. Fujita, *J. Am. Chem. Soc.* **2017**, *139*, 6090 – 6093; i) L. R. Holloway, P. M. Bogie, Y. Lyon, C. Ngai, T. F. Miller, R. R. Julian, R. J. Hooley, *J. Am. Chem. Soc.* **2018**, *140*, 8078 – 8081.
[15] a) C. W. Tornøe, C. Christensen, M. Meldal, *J. Org. Chem.* **2002**, *67*, 3057 – 3064; b) V. V. Rostovtsev, L. G. Green, V. V. Fokin, K. B. Sharpless, *Angew. Chem. Int. Ed.* **2002**, *41*, 2596 – 2599; *Angew. Chem.* **2002**, *114*, 2708 – 2711.
[16] B. Schulze, U. S. Schubert, *Chem. Soc. Rev.* **2014**, *43*, 2522 – 2571.
[17] R. A. S. Vasdev, D. Preston, J. D. Crowley, *Dalton Trans.* **2017**, *46*, 2402 – 2414.
[18] a) D. Zhao, S. Tan, D. Yuan, W. Lu, Y. H. Rezenom, H. Jiang, L. Q. Wang, H. C. Zhou, *Adv. Mater.* **2011**, *23*, 90 – 93; b) J. E. M. Lewis, C. John McAdam, M. G. Gardiner, J. D. Crowley, *Chem. Commun.* **2013**, *49*, 3398 – 3400; c) A. B. S. Elliott, J. E. M. Lewis, H. Van Der Salm, C. J. McAdam, J. D. Crowley, K. C. Gordon, *Inorg. Chem.* **2016**, *55*, 3440 – 3447; d) S. K. Samanta, J. Quigley, B. Vinciguerra, V. Briken, L. Isaacs, *J. Am. Chem. Soc.* **2017**, *139*, 9066 – 9074.
[19] B. M. J. M. Suijkerbuijk, B. N. H. Aerts, H. P. Dijkstra, M. Lutz, A. L. Spek, G. Van Koten, R. J. M. Klein Gebbink, *Dalton Trans.* **2007**, 1273 – 1276.
[20] An exception to this is the work of Crowley and co-workers who observed dramatic differences in the kinetics of self-assembly with triazole-based ligands dependent upon the nature of the *N*-substituent: S. Ø. Scott, E. L. Gavey, S. J. Lind, K. C. Gordon, J. D. Crowley, *Dalton Trans.* **2011**, *40*, 12117 – 12124.
[21] In the SCXRD structure of $[Pd(\mathbf{1})_4]^{2+}$ the complex is in an "all-up" conformation. If $[Pd(\mathbf{L}^{Phth})_4]^{2+}$ were to adopt this conformation exclusively in solution, the observed $H_a \cdots H_b$ NOESY cross-peaks would not be expected. It is assumed that in solution both mononuclear species are able to exist as rapidly interconverting conformers through rotation of the ligands about the Pd–N bonds.
[22] a) A. M. Johnson, O. Moshe, A. S. Gamboa, B. W. Langloss, J. F. K. Limtiaco, C. K. Larive, R. J. Hooley, *Inorg. Chem.* **2011**, *50*, 9430 – 9442; b) M. Frank, L. Krause, R. Herbst-Irmer, D. Stalke, G. H. Clever, *Dalton Trans.* **2014**, *43*, 4587 – 4592; c) M. Frank, J. Ahrens, I. Bejenke, M. Krick, D. Schwarzer, G. H. Clever, *J. Am. Chem. Soc.* **2016**, *138*, 8279 – 8287; d) F. J. Rizzuto, M. Kieffer, J. R. Nitschke, *Chem. Sci.* **2018**, *9*, 1925 – 1930; e) M. Kieffer, R. A. Bilbeisi, J. D. Thoburn, J. K. Clegg, J. R. Nitschke, *Angew. Chem. Int. Ed.* **2020**, *59*, 11369 – 11373; *Angew. Chem.* **2020**, *132*, 11465 – 11469.

Manuscript received: December 16, 2020
Accepted manuscript online: January 6, 2021
Version of record online: February 1, 2021

